

A NOVEL ENERGY-CONVERSION DEVICE FOR WIND AND HYDROKINETIC APPLICATIONS

Brent C. Houchens¹, David V. Marian
Sandia National Laboratories
Livermore, CA

Suhas Pol
Texas Tech University
Lubbock, TX

Carsten H. Westergaard
AeroMINE Power
Houston, TX

ABSTRACT

In its simplest implementation, patent-protected AeroMINE consists of two opposing foils, where a low-pressure zone is generated between them. The low pressure draws fluid through orifices in the foil surfaces from plenums inside the foils. The inner plenums are connected to ambient pressure. If an internal turbine-generator is placed in the path of the flow to the plenums, energy can be extracted. The fluid transports the energy through the plenums, and the turbine-generator can be located at ground level, inside a controlled environment for easy access and to avoid inclement weather conditions or harsh environments. This contained internal turbine-generator are the only moving parts in the system and are thus isolated from people, birds and other wildlife. The device could be used in distributed-wind energy setting, where the flow-directing, stationary foil pairs are located on warehouse rooftops, for example. Flow created by several such foil pairs could be combined to drive a common turbine-generator.

Keywords: AeroMINE, distributed wind, wind energy

NOMENCLATURE

A_{exit}	exit area (largest dimension) of unit
A_{jet}	total area of air-jets in foil surface
AoA	angle-of-attack (half-angle between foils)
CFD	computational fluid dynamics
$c_p(x)$	representation of surface pressure on foil
Δp	pressure-drop over jets and energy extraction
γ	representative jet discharge coefficient
L	chord length
LCOE	levelized-cost of electricity
Power	power of the AeroMINE unit
PIV	particle image velocimetry
PV	photovoltaic
ρ	air density
Re	Reynolds number
u_{jet}	flow velocity at air-jets
U_∞	free-stream velocity
V_{jet}	total volume flow through all air-jets

INTRODUCTION

Distributed wind energy has thus far failed to make a significant impact on the U.S. energy market [1]. Rotatory distributed wind turbines, in vertical or horizontal axis configurations, suffer from having many moving parts and associated vibration loads. For roof mounted systems, the standoff distances required for safe operation are significant. In all scenarios the swept area of distributed wind turbines is typically small, resulting in proportionally small power production.

AeroMINE (Motionless, INtegrated EXtraction) stationary wind harvesters provide safe, scalable, distributed electricity generation with no external moving parts as shown in Figure 1 for the wind-based configuration. When wind blows over AeroMINEs, low-pressure regions are created between pairs of foils that make up the body of the devices. These low-pressure

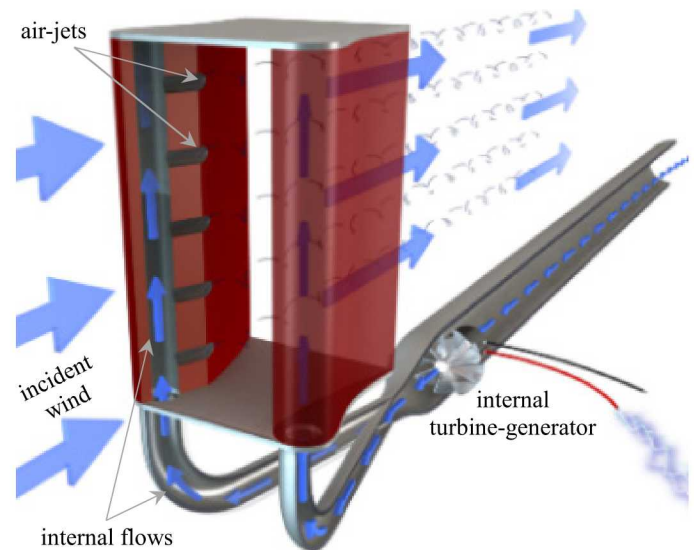


FIGURE 1: SCHEMATIC SHOWING THE OPERATION OF A SINGLE AEROMINE PAIR INCLUDING SEMI-TRANSPARENT/CUTAWAY FOILS AND INTERNAL AIR FLOW. (RENDERING BY VICENTE GARCIA)

¹ Contact author: brent.houchens@sandia.gov

regions suck air out of orifices (air-jets) in the surfaces of the foils. This air is pulled from ducts in the interior of the foils, through a manifold and over a coupled turbine-generator that produces electricity. The turbine-generator is located inside a controlled environment for easy access and to avoid inclement weather conditions. These are the only moving parts in the system and thus are isolated from people, birds and other wildlife.

Because AeroMINEs have no external moving parts, standoff distances for safety are eliminated and AeroMINEs can be scaled to large size as shown in the rendering in Figure 2a. This gives them large swept areas and proportional increases in power. They can easily integrate with existing buildings or operate stand-alone. Their patent-protected design [3, 4] is highly scalable and reliable, leading to significant, cost-effective power generation. At full implementation in viable locations across the U.S., AeroMINEs will safely, affordably and reliably power buildings and massively reduce emissions. In locations with strongly shifting wind directions, an optional yaw-control provides the ability to optimize power production, given that the building is still advantageously oriented over the range of wind directions. The system of multiple units can also complement distributed solar photovoltaics (PV) as shown in Figure 2c, providing power day and night.

1 PROJECT DESCRIPTION

AeroMINEs were designed by combining fast-iteration, moderate-resolution computational fluid dynamics (CFD) with 3D rapid prototyping and parameter optimization through wind tunnel testing. This allowed fast elimination of low performing designs and selection of the most promising configurations at the computational phase. Rapid prototyping with interchangeable components allowed affordable exploration of a range of the remaining designs. Wind tunnel tests at the Texas Tech University National Wind Institute provided optimum selection of air-jet locations and foil separation distances, as shown in the results in section 2.2. Experimental measurements included both duct velocities (at the turbine-generator location shown in Fig 2b) and particle image velocimetry (PIV) through the centerline of the AeroMINE foil-pair.

1.1 Design of Concept Unit for Wind Tunnel Tests

An S1210 airfoil was selected for the base design because it has good lift characteristics over a broad range of Reynolds numbers [2]. At or above Re of 200,000 (based on chord length) the S1210 can accept angles-of-attack (AoA) of up to 25° without experiencing stall. For a 1-m chord length AeroMINE in air at $20^\circ C$ and 1 atm, this allows for performance in as low as 3 m/s incident wind without stall.

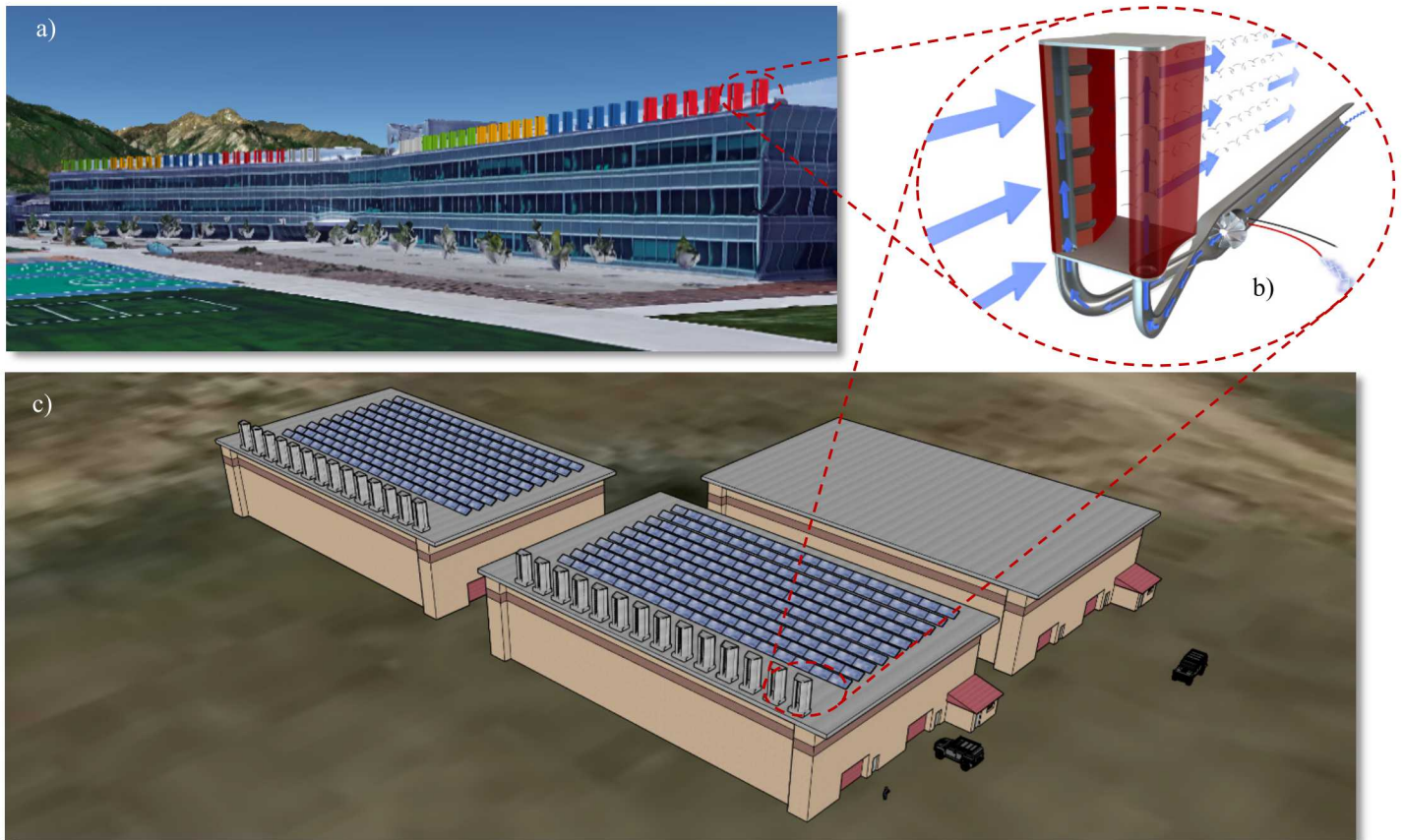


FIGURE 2: a) ARTIST RENDERING OF AN AEROMINE ARRAY ON AN OFFICE BUILDING (GOOGLE EARTH IMAGE), b) OPERATION OF A FOIL-PAIR, AND c) 14 AEROMINES AND 180 SOLAR PV PANELS ON 12,000 SQ.FT. WAREHOUSES WHERE THE SOLAR AND WIND SYSTEMS PRODUCE SIMILAR ENERGY PER YEAR FOR A SITE WITH BOTH FAVORABLE WIND AND SOLAR RESOURCES.

AeroMINES are characterized by a few basic geometric dimensions. The exit area A_{exit} is the height of the trailing edges multiplied by the distance between those edges, and is the largest overall dimension of the unit. By analogy with a horizontal axis wind turbine, this corresponds to the area swept by the rotor and provides the measure of total fluid from which the system can extract energy. The angle-of-attack (AoA) is the half-angle between foils, or the angle between the chord of either foil and the incident wind. Thus A_{exit} increases with increasing AoA. The total air-jet area A_{jet} is the sum-total of all the orifice areas in the surfaces of the two foils.

Simplified by assuming all jets perform the same, the air-jet discharged velocity can be related to the pressure difference from the inside of the foils as

$$\Delta p = \frac{1}{2} \cdot \rho \cdot c_p(x) \cdot U_\infty^2 = \frac{1}{2} \cdot \rho \cdot \frac{1}{\gamma} \cdot u_{jet}^2 \quad (1)$$

where $c_p(x)$ is a representative pressure created by the foils on their surface skin and γ is a representative loss coefficient including energy extraction. The power of the unit can then be computed from

$$Power = \Delta p \cdot V_{jet} \quad (2)$$

where the total volume flow through all the air-jets V_{jet} is

$$V_{jet} = u_{jet} \cdot A_{jet} \quad (3)$$

Substituting (1) for Δp into (2) gives

$$Power = \frac{1}{2} \cdot \rho \cdot c_p(x) \cdot U_\infty^2 \cdot V_{jet} \quad (4)$$

Or using (1) and (3) to eliminate u_{jet} gives

$$Power = \frac{1}{2} \cdot \rho \cdot c_p(x) \cdot U_\infty^2 \cdot A_{jet} \cdot \sqrt{c_p(x) \cdot \gamma} \cdot U_\infty \quad (5)$$

Normalizing the power with the maximum free stream power, $0.5\rho A_{exit} U_\infty^3$, based on the largest dimension of the unit, A_{exit} , allows comparison of the performance to Betz limit. After normalizing, equation (5) becomes

$$Coef_{power} = c_p(x)^{3/2} \cdot \sqrt{\gamma} \cdot \frac{A_{jet}}{A_{exit}} \quad (6)$$

Without measurements or high-fidelity CFD of the actual air-jet flow interaction with the external foil flow, or knowledge of the relationship between internal duct flow and energy extraction, it is not possible to determine γ in an analytic approach. However, these values can be correlated to wind tunnel measurements. For example, wind tunnel tests have shown $\gamma > 0.1$ can be achieved. The foil pressure $c_p(x)$ of two opposite foils can approach a coefficient of 4. The ratio $A_{jet}/A_{exit} > 0.2$ can likewise be achieved (albeit a much smaller ratio of 0.047 was used in the first results presented here). Using these possible values, a power coefficient of 51% is achievable, thus approaching Betz limit.

The initial air-jet design was based on a typical fixed wing vortex generator geometry in terms of slot spacing, angle orientation and repetition; whereas the area of the jets was determined based on a trade-off between the area needed to

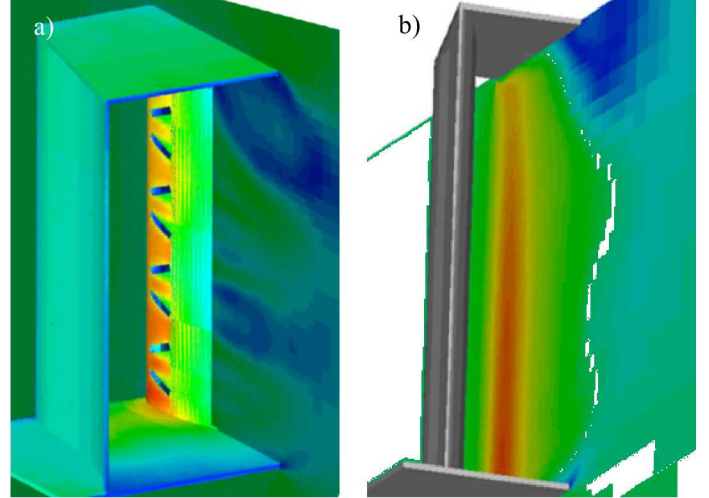


FIGURE 3: THREE-DIMENSIONAL CFD DESIGN RESULTS SHOWING a) VELOCITIES MAPPED ONTO AEROMINE SURFACES AND b) MIDLINE VELOCITY SPEEDUP.

generate a reasonable volume flow through device and disturbing the boundary layer on the foils.

1.2 Computational Fluid Dynamics Design

Coarse- and moderate-fidelity Euler based CFD was used to investigate the initial AeroMINE design and investigate foil spacing, air-jet placement and effects such as off-axis wind.

In Figure 3, the unit is placed on the wall to emulate the wind tunnel setup shown in Figure 4. In Figure 3b, the general centerline speed up is observed, which produces the low pressure between the two foils. In Figure 3a, the signature of the air-jets in the second jet slot pair from the bottom is clearly seen, but not in the first and the third. What appears to be the influence of the top plate is the signature of the jets, interacting with the top plate.

The CFD also demonstrated a range of effective values of angle-of-attack (10-25°) and spacing between a pair of foils (0.2L-0.8L) for chord length L . The test fixture was designed to accommodate flexibility in this range to complete the optimization with wind tunnel testing, as shown in Figure 4.

Additional simulations were performed to show the necessity of the top plate, and to investigate losses in the plenum and manifold, in which the turbine-generator is driven. CFD also indicated a potential instability which can break the symmetry of the flow and degrade performance. This was later observed experimentally in PIV measurements, but is reserved for a topic of a later paper.

1.3 Rapid Prototyping and Fixture Design

Foils and mounting blocks were rapid prototyped with interchangeable components for cost-effective testing. For example, several iterations of air-jets were tested by using removeable inserts in the foils. Thus, one set of foils was used to test many configurations of air-jets. The air-jet inserts printed approximately 10 times faster than the foils.

The foils shown in Figure 4c have chord $L=25$ cm and are 40 cm tall. Spacer blocks in increments of 25 mm were also

rapid prototyped to allow investigation of a range of foil spacings. Mounting blocks with 5° increments in AoA allowed fast and reproducible changes, without the need to modify the manifold. They also accommodate off-preferential wind direction testing. These mounting blocks and spacers adapted to aluminum rails which make up the backbone of the fixture, as shown in Figure 4a. A clear plexiglass top was constructed to accommodate PIV imaging of the flow between the foils.

Multiple pairs of AeroMINES can be mounted in parallel (as shown in Figure 4c). This allowed testing of the influence of between-pair spacing. Furthermore, a second row of AeroMINES can be mounted behind the first, to investigate the impact of a wake from upstream foils on downstream energy production. Though not a focus of this paper, ongoing testing is investigating the feasibility of using an entire roof, rather than just the leading edge.

1.4 Wind Tunnel Testing

The test fixture, designed to ensure reproducibility of experiments, was installed at the Texas Tech University National Wind Institute wind tunnel as shown in Figure 4. The section of the tunnel shown is 4-feet high by 6-feet wide. Testing on scaled, 3D rapid prototyped models was performed at 10 m/s and 15 m/s freestream velocities, corresponding to Re of 170,000 and 255,000, respectively. This testing verified optima in performance (based on duct velocity) both in angle-of-attack and spacing between foil pairs. Additionally, PIV measurements were taken to better understand the acceleration between the foils and the wake structure.

A vane anemometer was mounted in the combined inlet duct (1-inch PVC) at the location of the turbine-generator and the average duct velocities were measured. The inlet flow was choked to simulate the turbine-generator under various loading conditions.

2 RESULTS

Initial computational and experimental results are given here for the first-generation (1st-gen) design, which is shown in Figure 4. Sample costs of electricity based on an improved second generation (2nd-gen) design are then compared to solar photovoltaics.

2.1 Computational and Experimental Results for 1st-Gen Design

Three-dimensional CFD simulations of multiple pairs of AeroMINES are shown in Figure 5. To avoid a blockage effect, the pairs must be spaced sufficiently far apart. For this design, an optimum spacing of approximately the exit width is observed as shown in Figure 5a. Figure 5b shows the advantageous rooftop speedup for a large format building such as a warehouse or box store with an array of AeroMINES. When the building faces the dominant wind direction, the flow up and over the building can greatly enhance the performance of the array.

A sample of time-averaged PIV data is shown in Figure 6 for a 15 m/s freestream. Note that the pins that hold on the top plate (see Figure 4c) create two obstacles for the cameras and

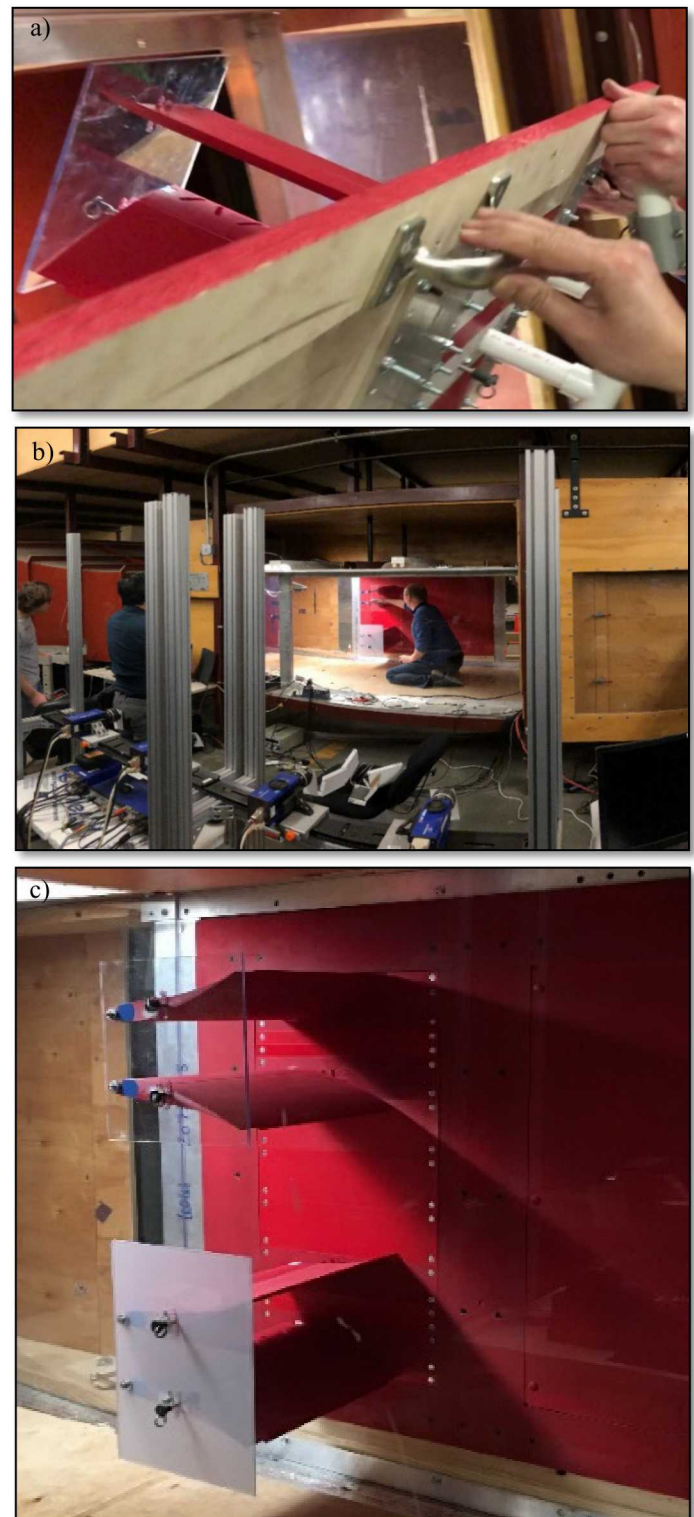


FIGURE 4: THE MODERATE TURBULENCE INTENSITY WIND TUNNEL AT TEXAS TECH UNIVERSITY, SHOWING a) CLOSE-UP OF THE TEST FIXTURE WHICH ALLOWS OPTIMIZATION ON AOA AND SPACING b) THE LASER VELOCIMETRY CAMERA ARRAY, c) TWO 1ST-GENERATION BENCH-SCALE AEROMINES IN THE TEST FIXTURE IN PARALLEL.

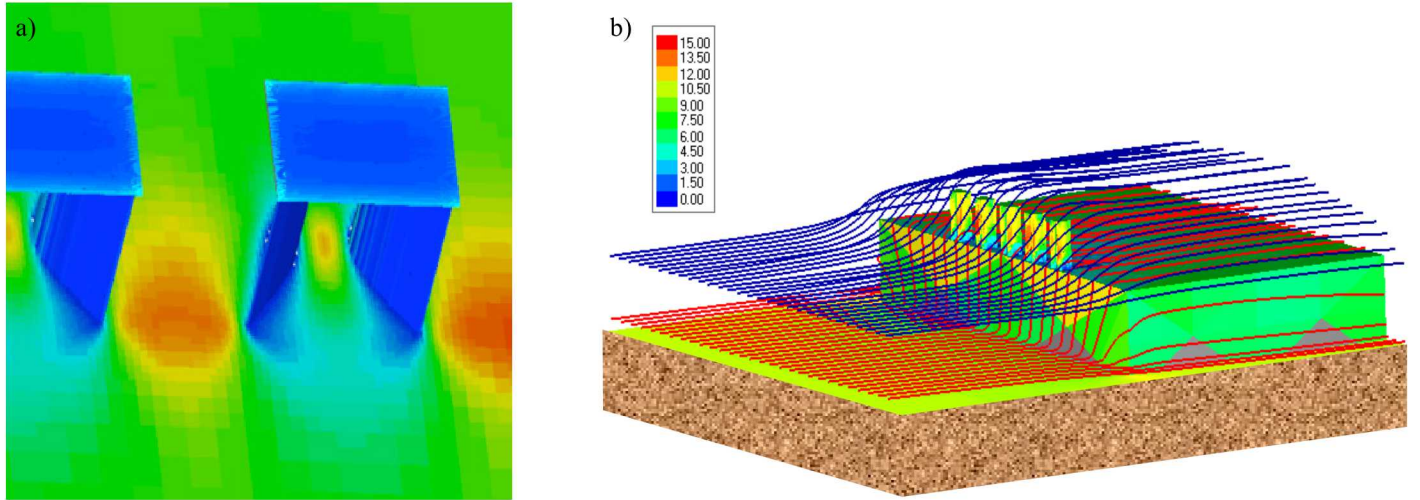


FIGURE 5: THREE-DIMENSIONAL CFD RESULTS SHOWING A) OPTIMIZATION OF BETWEEN-PAIR SPACING AND B) ROOFTOP SPEEDUP EFFECT SEEN BY A ROOF-MOUNTED ARRAY DUE TO A BUILDING.

appear as regions of no velocity near the foil surfaces. The speedup between the foils is nearly double that of the freestream, creating a very low-pressure region that sucks air out of the air-jets. In this scenario the wake is symmetric and performance is balanced.

The optimization on AoA is shown in Figure 7 based on the measured duct velocity at the location of the turbine-generator. At 10 m/s freestream ($Re = 170,000$) the optimum at 15° is very apparent in the unloaded (open) scenario. Over a 50% speedup in the duct is measured over the freestream. By 20° the performance is greatly reduced due to separation of the flow.

Note that this Re is below the design target of 200,000 to avoid such stall effects. When the system is choked the duct velocity is reduced, providing a surrogate model of a power curve for the device.

At 15 m/s freestream ($Re = 255,000$) the performance is roughly the same at 10° and 15° AoA. At 15° AoA the swept area is larger, providing more potential energy. In the choked condition the system performs equally well between 10° and 20° AoA. This consistency provides the opportunity to optimize on a multifoil array, rather than on an individual pair, which is a topic for a future paper.

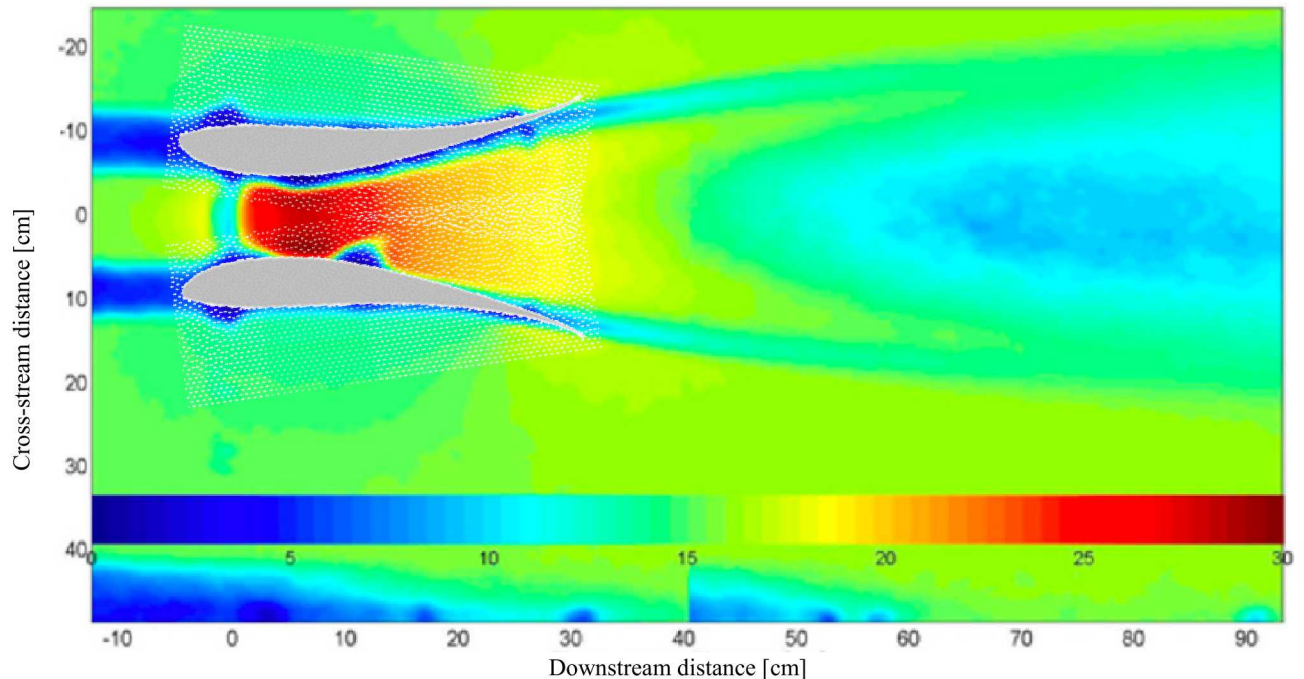


FIGURE 6: PARTICLE IMAGE VELOCIMETRY DATA IN A PLANE ALIGNED WITH THE CHORD FOR 15 M/S FREESTREAM VELOCITY.

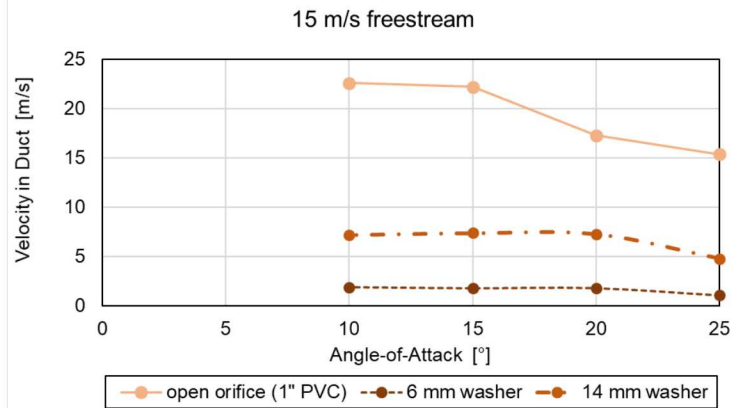
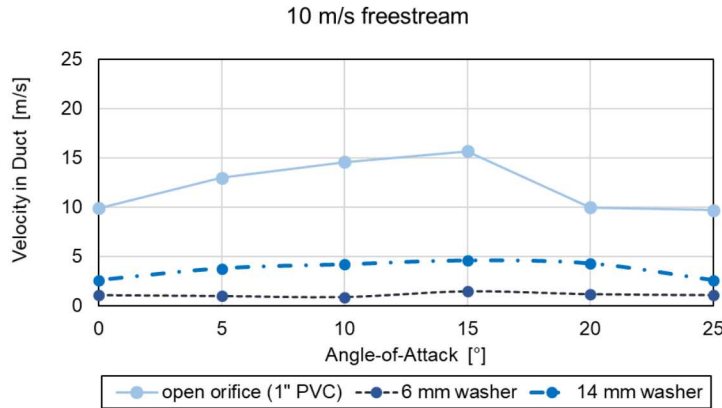


FIGURE 7: EXPERIMENTALLY MEASURED DUCT VELOCITY AT LOCATION OF TURBINE-GENERATOR FOR VARIOUS AOA FOR 10 M/S AND 15 M/S FREESTREAM VELOCITIES SHOWING OPTIMUM OPERATIONS NEAR 15° AOA.

2.2 Cost of Energy Estimates for 2nd-Gen Design

Utility-scale wind turbines sell for \$1071/kW [5]. The levelized-cost of electricity (LCOE) of utility scale wind is now competitive with natural gas at around 5 ¢/kWh. However, utility scale wind is not viable in all areas, even where wind resources are prevalent. For example, around existing built environments and cities it is often impractical or impossible to retrofit utility scale turbines. In these environments, a distributed wind solution is needed.

To estimate the LCOE of AeroMINEs, typical installation costs of solar PV panels on commercial building rooftops was assumed [6] and rescaled to the current industry standards. AeroMINEs would require almost identical installation methods. This analysis shows that AeroMINEs can be installed at \$2,400/kW. Finally, at optimum performance AeroMINE systems can reach a LCOE of 10 ¢/kWh at just over 5 m/s average annual wind speed, which is highly competitive with a solar PV installation. At higher wind speeds, even lower cost of energy is reached. Future pilot-scale testing is needed to verify this LCOE estimate. It will also be critical to create methodologies to provide detailed wind energy resource assessments in complex built environments.

3 CONCLUSIONS

This work provides a proof-of-concept demonstration of AeroMINE distributed wind energy harvesters. Levelized-cost-of-energy has been estimated and shown to be very competitive with solar panels on commercial rooftops. AeroMINEs potential to provide renewable power in a scalable, safe, and reliable system has the potential to significantly impact the untapped distributed wind energy space. AeroMINEs can also be co-installed with solar PV for locations with favorable wind and solar resources.

ACKNOWLEDGEMENTS

Sandia National Laboratories is a multimission laboratory managed and operated by National Technology & Engineering Solutions of Sandia, LLC, a wholly owned subsidiary of Honeywell International Inc., for the U.S. Department of Energy's National Nuclear Security Administration under contract DE-NA0003525. The views expressed in the article do not necessarily represent the views of the U.S. Department of Energy or the United States Government.

REFERENCES

- [1] *2016 Distributed Wind Market Report*, U.S. Department of Energy Office of Energy Efficiency and Renewable Energy.
- [2] Selig, M.S., Guglielmo, J.J., Broeren, A.P. and Giguere, P. *Summary of Low-Speed Airfoil Data*, Vol. 1, 1995.
- [3] Westergaard, C.H., *Fluid flow energy extraction system and method related thereto*, US2017298900, US Patent Office.
- [4] Houchens, B.C., Blaylock, M.L., Marian, D.V. Maniaci, D.C. and Westergaard, C.H., *Methods, systems, and devices to optimize a fluid harvester*, priority app US 16/182,488, 2018.
- [5] Stehly, T. Heimiller, D. and Scott, G., *2016 Cost of Wind Energy Review*, Technical Report NREL/TP-6A20-70363 December 2017.
- [6] Fu, R. Chung, D., Lowder, T., Feldman, D., Ardani, K. and Margolis, R., *U.S. Solar Photovoltaic System Cost Benchmark: Q1 2016*, Technical Report NREL/TP-6A20-66532.